

The Locus of the apices of projectile trajectories under constant drag

H. Hernández-Saldaña

Departamento de Ciencias Básicas,

Universidad Autónoma Metropolitana at Azcapotzalco,

Av. San Pablo 180,

México 02200 D.F., Mexico.

(Dated: May 31, 2017)

We present an analytical solution for the projectile coplanar motion under constant drag parametrised by the velocity angle. We found the locus formed by the apices of the projectile trajectories. The range and time of flight are obtained numerically and we find that the optimal launching angle is smaller than in the free drag case. This is a good example of problems with constant dissipation of energy that includes curvature, and it is proper for intermediate courses of mechanics.

I. INTRODUCTION

Projectile trajectory under constant drag has deserved a lot of attention in literature, not only as it appears as a common problem in undergraduate physics and can be given recent exact analytical results and new analysis[1–5]. The power-law velocity dependent drag

$$\vec{f} = - \sum_n mgb_n v^n \frac{\vec{v}}{v}, \quad (1)$$

with $v = ||\vec{v}||$, is a series approximation for the real complex problem. The linear, $n = 1$, and quadratic, $n = 2$, cases are of much used, not only for the analysis of the motion of a particle in midair but as well to model other energy dissipation process. In the quantum scales, $n = 1$ is a usual model for the energy losses[6, 7].

Notwithstanding the usefulness of linear approximation, and that allows analytical solutions for the projectile motion, equation (1) have an-

other case: $n = 0$, the constant drag case. It is not trivial if, as it is usual, the projectile motion is coplanar, i.e., the vector \vec{v}/v changes with the orientation of the orbit.[21] This case has deserved few attention, the only reported work we found are [8, 9].

There is not evidence that exists a regime where the drag could be considered constant, however the problem studied here is important for the following reasons:

i) A series expansion for a retarding force has to have a no null zeroth term, take for instance, the integrable Legendre cases

$$f(v) = \frac{1}{n}(a + bv^n), \quad (2)$$

where the constant $a \neq 0$ appears[10]. ii) The motion of an object in a non-newtonian fluid with yield stress could be constant, see for instance [11], i.e., the problem of a particle launched in oil or liquid chocolate contains

this constant term. Even more, spheres into loose granular media are another example of an object moving in a fluid with presence of yield stress[12]. iii) As an undergraduate problem, a constant retarding force could be considered as a point rocket with the thrust pointed against the motion. iv) As a simple example of friction that depends on the curvature.

In the present paper we analyse such a case, obtaining both the explicit solutions of the problem in the next section and the description of the locus which give title to this work. We discuss the range and the time of flight are given in section IIIB. Conclusions are presented in section IV.

II. THE PROJECTILE PROBLEM WITH CONSTANT DRAG

The constant drag problem is governed by the following equations in rectangular coordinates

$$m \frac{d^2}{dt^2} \vec{r} = -mg\hat{j} - mgb_0 \vec{v}/v. \quad (3)$$

Notice that the friction is constant *in the direction of motion*, i.e., it changes with velocity. We choose the drag force in units of weight mg in order to compare with linear and quadratic drag results.

In order to be clear on what kind of differential equations we are dealing with, we explicitly rewrite the above equations in cartesian coordi-

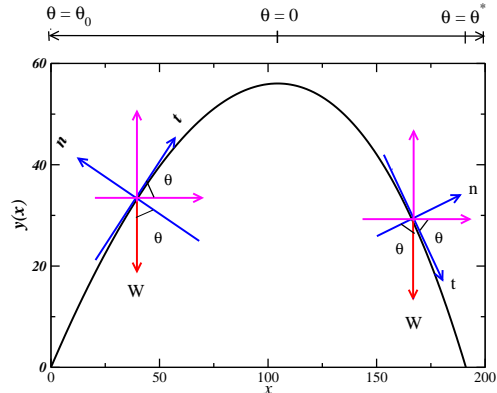


FIG. 1: (color online) The normal, n , and tangent, t , reference frame during the projectile movement (in blue lines) as comparison to the usual reference frame $x - y$ (in magenta lines). The first comparison previous to reaching the apex and the second, afterward. In the upper scale we show the velocity angle scale θ starting at θ_0 up to the angle when $y = 0$, i.e., $-\theta = \theta^*$. The final, asymptotic, angle is $\theta = -\pi/2$, regardless the value of the dissipation parameter. As usual, $W = mg$, indicated in red. Plotted trajectory corresponds to $v_0 = 50$, $\theta_0 = \pi/4$ and $b_0 = 0.25$ in SI units.

nates

$$\begin{aligned} m\ddot{x} &= -mgb_0 \frac{\dot{x}}{\sqrt{\dot{x}^2 + \dot{y}^2}}, \\ m\ddot{y} &= -mg - mgb_0 \frac{\dot{y}}{\sqrt{\dot{x}^2 + \dot{y}^2}}. \end{aligned} \quad (4)$$

Here, we use a dot for a time derivative. The above equations are coupled and non-linear. However an analytical solution parametrised with the velocity angle can be obtained. Some other results require of standard numerical methods[13]. The solutions presented here for x and y do not require of any further numerical integration.

III. EXPLICIT SOLUTION PARAMETRISED BY θ .

In order to obtain a solution of the problem (4) we first change the equations for normal, n , and tangent, t , coordinates to the motion, hence, the corresponding force components are

$$F_t = -mg \sin \theta - mgb_0, \quad (5)$$

and

$$F_n = -mg \cos \theta. \quad (6)$$

If the mass is constant, we obtain

$$m\dot{v} = -mg \sin \theta - mg - mgb_0 \quad (7)$$

and

$$m \frac{v^2}{\rho} = -mg \cos \theta. \quad (8)$$

where $\rho = -ds/d\theta$ and, s is the arc length. The last equation can be written as

$$v\dot{\theta} = -g \cos \theta, \quad (9)$$

with the help of the chain rule: $\rho = -ds/d\theta = -(ds/dt)(dt/d\theta)$. Equation (7) for the tangent

acceleration can be modified with the same rule and using (9) the result is

$$\frac{dv}{d\theta} = v(\tan \theta + b_0 \sec \theta). \quad (10)$$

For the initial conditions $v(t = 0) = v_0$ and $\theta(t = 0) = \theta_0$, we solve this first order differential equation obtaining

$$v(\theta) = \frac{v_0 \cos \theta_0}{\cos \theta} \left(\frac{\Delta}{\Delta_0} \right), \quad (11)$$

with

$$\Delta \equiv (\sec \theta + \tan \theta)^{b_0},$$

and $\Delta_0 \equiv \Delta(\theta_0)$.

The solution for time is

$$\begin{aligned} t(\theta) &= -\frac{1}{g} \int_{\theta_0}^{\theta} v(\theta) \sec \theta d\theta \\ &= -\frac{v_0 \cos \theta_0}{g \Delta_0} \left(\frac{(b_0 - \sin \theta) \Delta}{(b_0^2 - 1) \eta} - \frac{(b_0 - \sin \theta_0) \Delta_0}{(b_0^2 - 1) \eta_0} \right), \end{aligned} \quad (12)$$

being

$$\eta = (\cos \theta/2 - \sin \theta/2)(\cos \theta/2 + \sin \theta/2), \quad (13)$$

and $\eta_0 \equiv \eta(\theta_0)$.

Using a similar procedure we obtain

$$\begin{aligned} x(\theta) &= -\frac{1}{g} \int_{\theta_0}^{\theta} v(\theta)^2 d\theta \\ &= -\frac{1}{g} \left(\frac{v_0 \cos \theta_0}{\Delta_0} \right)^2 \left[-\frac{(-2b_0 + \sin \theta) \Delta^2}{(2b_0 - 1)(2b_0 + 1) \eta} + \frac{(-2b_0 + \sin \theta_0) \Delta_0^2}{(2b_0 - 1)(2b_0 + 1) \eta_0} \right], \end{aligned} \quad (14)$$

and

$$\begin{aligned}
y(\theta) &= -\frac{1}{g} \int_{\theta_0}^{\theta} v(\theta)^2 \tan \theta d\theta \\
&= -\frac{1}{g} \left(\frac{v_0 \cos \theta_0}{\Delta_0} \right)^2 \left[\frac{\sec^2 \theta (-3 + \cos 2\theta + 4b_0 \sin \theta) \Delta^2}{8(b_0^2 - 1)} \right. \\
&\quad \left. - \frac{\sec^2 \theta_0 (-3 + \cos 2\theta_0 + 4b_0 \sin \theta_0) \Delta_0^2}{8(b_0^2 - 1)} \right].
\end{aligned} \tag{15}$$

So, (12),(14) and (15) are, formally, the solutions to the problem (4). Unfortunately, explicit inversion of $t(\theta)$ is hard (if not imposible). Notwithstanding, these solutions are analytical and no additional integration is required. In search of an explicit time dependent solution homotopy analysis method could offer a guide as it was the case of quadratic drag [1].

In order to establish that previous expressions are as useful as the time parametrisation we shall use them to plot the usual graph of $x(t)$ and $y(t)$ as well as the iconic $y(x)$ (see 2). For comparison, we rewrite the free drag solutions as function of θ , the results

$$t(\theta) = -\frac{v_0 \cos \theta_0}{g} (\tan \theta - \tan \theta_0), \tag{16}$$

$$x(\theta) = -\frac{(v_0 \cos \theta_0)^2}{g} (\tan \theta - \tan \theta_0), \tag{17}$$

and

$$y(\theta) = -\frac{(v_0 \cos \theta_0)^2}{2g} (\sec^2 \theta - \sec^2 \theta_0), \tag{18}$$

are obtained by solving (7) and (8) for $b_0 = 0$.

It is an exercise to check that the previous expression are the familiar solutions of parabolic motion.

First we explain the solutions in angle parametrisation. To this end we draw equation

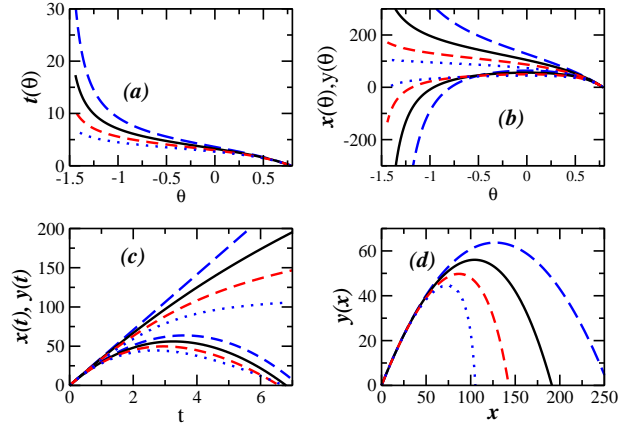


FIG. 2: (color online) Explicit solution to the projectile motion in presence of a constant drag as function of the angle θ , in all cases we draw the drag-free solution in blue broken lines, $b_0 = 0.25$ in black lines, $b_0 = 0.5$ in red dashed lines and the blue dotted lines correspond to $b_0 = 0.75$. In (a) time is depicted, notice that the angle go from θ_0 to $-\pi/2$ as time increases. In (b) we shown x and y as function of the angle, functions that growing to ∞ correspond to x and those going to $-\infty$ are for y solutions. In (c) and (d) we depict the solution in the traditional variables, x and y as function of time for the former and y as function of x in the latter.

(12) in figure 2(a), i.e., time as function of θ for $b_0 = 0.25$ (black line), $b_0 = 0.5$ (red dashed line) and $b_0 = 0.75$ (blue dotted line) and the free drag case in blue dashed line, from (16). The launching angle was set to $\theta_0 = \pi/4$ here, other

selection shall shift the graphs (not shown). The parameter θ go, asymptotically, to $-\pi/2$, since the reference frame change the orientation after the orbit reach its apex as it appears in figure 1.

In figure 2b) solutions (14) for $x(\theta)$ are presented in the same order as before (graphs diverging to ∞ as $\theta \rightarrow -\pi/2$). The solutions (14) for $y(\theta)$ are those that diverge to $-\infty$ as $\theta \rightarrow -\pi/2$. A close up of them (not shown) could show the angle where $y = 0$. The numerical solutions to this condition shall be discussed below. Again we draw in blue-dashed lines the drag free solutions from (17) and (18).

In figure (2)c) time solutions are presented for $x(t)$ (upper graphs) and $y(t)$ (lower graphs). Using (14), (15) and a simple computational program we can write the $x(t(\theta))$ and $y(t(\theta))$ data and plot it. We do that and we present the results for the same drag values and color code. We consider only the range of θ in order to show the $y = 0$ condition. The y results show the larger the drag the shorter the maxima. The maxima are reached at a shorter times as the drag increases, as well.

Finally, we present the iconic $y(x)$ for projectile motion in figure (2)d). As expected, the larger the b_0 value the shorter the path. Certainly, at first sight the paths are similar to those obtained with a linear drag, but a comparison require to compare energy losses, not similar val-

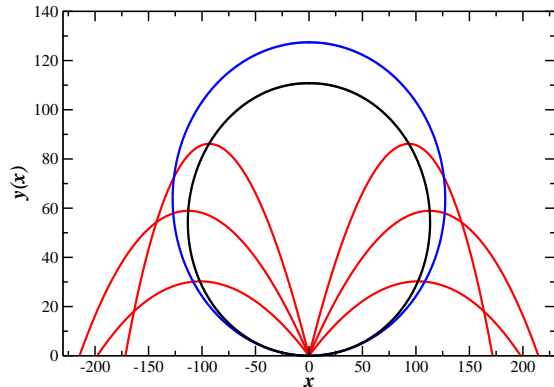


FIG. 3: (color online) Locus formed by the apices of all the projectile trajectories for constant drag with the same initial speed (black line). In blue broken lines the solution for the free drag case. The parameters used here are $v_0 = 50$, $b_0 = 0.15$ and we plot in red the trajectories for $\theta_0 = 30^\circ$, $\theta_0 = 45^\circ$ and $\theta_0 = 60^\circ$.

A. The locus of the apices

The solution in terms of the angle could be hard to handle but gives a straightforward for a particular locus: the locus formed by all the apices for initial launching angle θ_0 . The cases for no drag[15–17] and linear drag has been studied previously[18–20].

The apex for each orbit is obtained by setting $\theta = 0$ for x and y in (14) and (15) as can be seen at figure (1). After rearranging factors in these equations and using $(\cos \theta_0/2 - \sin \theta_0/2)(\cos \theta_0/2 + \sin \theta_0/2) = \cos \theta_0$ [22], the locus is written as

$$x(\theta_0) = -\frac{1}{g(4b_0^2 - 1)} \left(\frac{v_0 \cos \theta_0}{\Delta_0} \right)^2 \left[2b_0 + \frac{(-2b_0 + \sin \theta_0) \Delta_0^2}{\cos \theta_0} \right] \quad (19)$$

and

$$y(\theta_0) = \frac{1}{8g(b_0^2 - 1)} \left(d \frac{v_0 \cos \theta_0}{\Delta_0} \right)^2 \left[2 + \sec^2 \theta_0 (-3 + \cos 2\theta_0 + 4b_0 \sin \theta_0) \Delta_0^2 \right]. \quad (20)$$

In figure (3) we show the locus for parameters with values $v_0 = 50$ m/s, $b_0 = 0.15$ and $g = 9.81$ m/s². The drag-free solution

$$x_m = \rho \sin \theta_0 \cos \theta_0, \quad (21)$$

$$y_m = \frac{\rho}{2} \sin^2 \theta_0, \quad (22)$$

is shown for comparison. We add three orbits, those corresponding to launching angles $\theta_0 = 30^\circ$, $\theta_0 = 45^\circ$ and $\theta_0 = 60^\circ$ as is usual in the textbooks.

B. Some important quantities in projectile motion: The range and the flight time

Unfortunately not all the important quantities are of mathematical significance. Meanwhile the apex has a mathematical meaning, other locus are important for practical reason. Such is the case of the range and its maximum. Their

value are determined by our choose of the origin

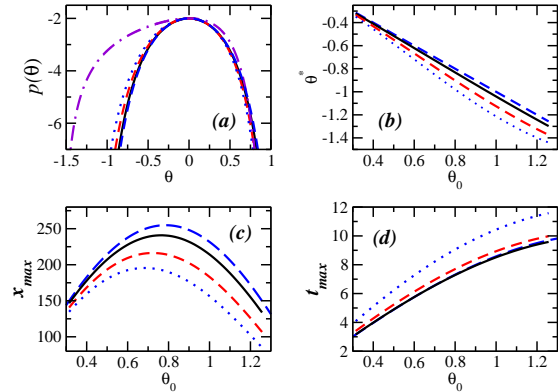


FIG. 4: (color online) Range, x_{max} , and flying time

the origin is determined in an arbitrary way and hence the length of the chord. Hence, it is not surprising that we need to solve numerically (15) for $y = 0$.

This condition is translated from (15) to solve the equation

$$\sec^2 \theta (-3 + \cos 2\theta + 4b_0 \sin \theta) \Delta^2 = \sec^2 \theta_0 (-3 + \cos 2\theta_0 + 4b_0 \sin \theta_0) \Delta_0^2 \quad (23)$$

If we call $p(\theta) = \sec^2 \theta (-3 + \cos 2\theta + 4b_0 \sin \theta) \Delta^2$, we are looking for solutions such that $p(\theta) = p(\theta_0)$. For symmetrical functions the solutions is clear, but this is not the case as can be seen in figure 4a). There we plot p for the indicated values of b_0 and the free-drag case $\sec^2 \theta (-4 + 2 \cos^2 \theta) = \sec^2 \theta_0 (-4 + 2 \cos^2 \theta_0)$ with the solution $\theta^* = \pm \theta_0$ (in blue dashed line). In this figure the drag values considered are $b_0 = 0.05$ in black line, 0.15 in red dashed line and 0.25 in dotted blue line. We add the extreme case of $b_0 = 0.75$ in order to show how asymmetric the curve $p(\theta)$ can be[23]. The color code remains in the rest of the graphs.

In figure 4b) we show the solution obtained via Newton-Raphson for the equation $p(\theta^*) - p(\theta_0) = 0$ and the corresponding case for the range $x_{max} = x(\theta^*)$ as function of the launching angle in figure 4c).

In the last figure the maximum range occurred at $\theta_0 \approx 0.7697, 0.7226$ and 0.6912 for the indicated values of b_0 . All these values are smaller than $\theta_0 = \pi/4 \approx 0.7854$, the corresponding value for the drag free case (shown in blue broken line). For completeness, we present the time of flight as function of the launching angle in figure 4(d). Such a time increases with the angle. Notice that the drag free case and the so-

lution for $b_0 = 0.05$ are so close that they appear superimposed.

IV. CONCLUSIONS

We discussed the motion of a projectile under the influence of constant gravitational pull and constant drag. Such a case could be considered as the yield stress in a non-newtonian fluid and as an example of a simple situation where the retarding force depends on the velocity direction. The two coupled non-linear differential equations in rectangular coordinates can be exactly solved by a change to normal and tangent coordinates. The solutions, (14) and (15), are parametrised as functions of the velocity angle. That allow us to obtain the locus of the apices in an explicit way. Other locus or quantities require of numerical calculation as the range and flight time presented in the previous section.

This problem serves as a good example for introduce undergraduate students to problems with curvature and retarding forces, beyond the problem of an inclined plane with constant friction.

Acknowledgment

We thank to AL Salas-Brito for valuable comments.

References

-
- [1] Yabushita K, Yamashita M and Tsuboi K 2007 *J Phys A: Math and Theo* **40** 8403–8416 ISSN 1751-8113
- [2] Belgacem C H 2014 *Eur J Physics* **35** 055025
- [3] Turkyilmazoglu M 2016 *Eur J Phys* **37** ISSN 0143-0807
- [4] Morales D A 2016 *Acta Mech* **227** 1593–1607 ISSN 0001-5970
- [5] Stewart S M 2012 *Eur J Phys* **33** 149–166 ISSN 0143-0807
- [6] Dittrich T, Hänggi P, Ingold G L, Kramer B, Schön G and Zwerger W 1998 *Quantum Transport and Dissipation* (Wiley-VCH) ISBN 978-3527292615
- [7] Razavy M 2006 *Classical and Quantum Dissipative Systems* (Imperial College Press) ISBN 9781783260393
- [8] Jones S E, Caipen T L and Butson G J 1991 *International Journal of Applied Engineering Education* **7** 321–327
- [9] Jones S E 1991 The projectile motion problem including the effects of constant thrust and drag *Challenges of a changing world* vol 1 and 2 ed Educ A S E The organization (Univ. of New Orleans, New Orleans, LA: Amer. Soc. Engineering Education) pp 1839–1841 proceeding paper
- [10] MacMillan W 1927 *Theoretical Mechanics: Static and the Dynamics of a Particle* (McGraw-Hill)
- [11] Barnes H A 1999 *J Non-Newt Fluid Mech* **81** 133–178
- [12] Bruyn J R and Walsh A M 2004 *Can. J. Phys.* **82** 439446
- [13] Burden R L, Faires J D and Burden A M 2015 *Numerical Analysis* (Brooks Cole)
- [14] Hernández-Saldaña H Energy losses in projectile motion under constant, linear and quadratic drag work in progress
- [15] Fernández-Chapou J L, Salas-Brito A L and Vargas C A 2004 *Am J Phys* **72** 1109 ISSN 0002-9505
- [16] Thomas G, Weir M, Hass J and Giordano F 2004 *Calculus* (Addison-Wesley)
- [17] Carrillo-Bernal M A, Mancera-Piña P E, Cerecedo-Nuñez H H, Padilla-Sosa P, Nuñez Yépez H N and Salas-Brito A L 2014 *Am. J. Phys.* **82** 707 ISSN 0002-9505
- [18] Stewart S 2006 *Int J Math Educ Sci Technol* **37** 411–431
- [19] Stewart S M 2011 *Eur J Phys* **32** L7–L10 ISSN 0143-0807
- [20] Hernández-Saldaña H 2010 *Eur J Physics* **31** 1319–1329
- [21] In one dimension this term only changes the sign of the force in order to keep it in opposition to the movement.
- [22] Since the launching angle remain in the first quadrant
- [23] Calculations for values of b_0 larger than 0.25 require of a better selection of the initial condition as we can be seen for $b_0 = 0.75$ in figure 4(a)